

Continuous-wave laser-pumped optical bistability in thermally deposited and molecular-beam-grown ZnSe interference filters

Y. T. Chow, B. S. Wherrett, E. Van Stryland,* B. T. McGuckin, D. Hutchings, J. G. H. Mathew, A. Miller, and K. Lewis†

Department of Physics, Heriot-Watt University, Edinburgh EH14 4AS, United Kingdom

Received March 30, 1986; accepted July 30, 1986

We observe and compare conditions for cw optical bistability in both thermal-vacuum-deposited and molecular-beam grown ZnSe-based interference filters, at He-Ne-laser (633-nm), Kr (647-nm), and Ar-ion (514-nm) wavelengths. Bistability is observed at 514 and 647 nm and, by inference, should be observable at a number of intervening wavelengths for a single molecular-beam-grown sample. From our theoretical analysis we also demonstrate that observed drift instabilities in filter nonlinear responses correlate with the highest internal irradiance levels.

INTRODUCTION

The prospect of fabricating optically bistable and transphaser plates for optical array processing, spatial light modulation, and displays has led to considerable recent interest in multilayer dielectric nonlinear interference filters. Specifically, cw optical bistability has been investigated at Ar-ion laser wavelengths, using narrow-bandpass filters that operate as high-finesse Fabry-Perot systems.^{1,2} Reports of modulated-Ar experiments^{3,4} and of dye-laser-pumped bistability in filters have also been made.⁵

A theoretical study of the critical switching condition that determines the characteristic irradiance or power level for bistability⁶ led to predictions of optimum cavity parameters for low-power switching. In the present paper we report investigations of (1) filters produced entirely by thermal vapor deposition in conventional high vacuum, with approximately 500-nm-thick spacer regions, and (2) filters with spacers of thickness up to 6.6 μm , grown by the molecular-beam (MB) technique in ultrahigh vacuum. The switching power levels are shown to be consistent with theory. They are low enough to permit use of a 30-mW cw He-Ne laser and lead to predictions of stable, submilliwatt switching of 20- μm spot-size beams in fully optimized samples. A comparison with Ar-ion results is made.

FILTER CONSTRUCTION

The thermally evaporated filters used consisted of ZnSe spacers, two optical wavelengths thick, surrounded by high-reflectivity stacks. Each stack consisted of four high-low layer pairs, the high-index material being ZnSe and the low-index ThF₄. The results described herein were achieved for filters with a normal incidence transmission peak at 635 nm. For the He-Ne 633-nm line, a low-power transmission maximum of 73% was achieved at an incident angle of 13°. A passive (linear) transmission analysis implies a ZnSe loss coefficient of 110 cm^{-1} . This result is consistent with the

wavelength dependence of the loss, as determined from a number of filter and single thin-film samples. The thermally deposited ZnSe structure is far from single crystal, and loss coefficients considerably higher than those in the bulk material are obtained in the films in the band-tail spectral region.

To produce samples with thicker spacers so that bistability could be investigated over a range of wavelengths in a single sample, a MB-deposited layer was grown between reflective stacks each of two high-low thermally deposited layers of ZnSe-ThF₄. The MB evaporation was carried out in an ultrahigh-vacuum system⁷ at pressures P_T in the range 2 to 8×10^{-9} mbar. Residual gas analysis revealed the dominant permanent gas species present to be H₂ (partial pressure of $0.97P_T$) with minority species CO ($0.02P_T$), Ar ($0.01P_T$), CH₄ ($0.004P_T$), and H₂O ($0.001P_T$). The ZnSe films were deposited onto unheated substrates (30–40°C) at growth rates in the range of 0.6–0.9 μm per hour, from a stoichiometric beam of Zn and Se₂ molecular species. No attempt was made to correct for inequality in the sticking coefficients of the separate Zn and Se₂ species. The molecular beam was generated from a single Knudsen cell source containing ultrahigh-purity polycrystalline ZnSe that had previously been prepared by chemical vapor deposition from a mixture of Zn vapor and H₂Se.⁸ Typical ZnSe source temperatures were in the range 910–960°C.

Figure 1(b) shows the filter transmission over the 500–800-nm range, for a sample of 6.6- μm spacer thickness, compared with a thin-spacer case [Fig. 1(a)]. By using a small wedge angle in the spacer, the MB filters could be translated to bring one of the normal incidence transmission maxima to the desired detuning from a given laser line, for diagnostic purposes.

THERMAL CHARACTERIZATION

The temperature dependence of the ZnSe refractive index is considered to be the dominant cause of nonlinear transmis-

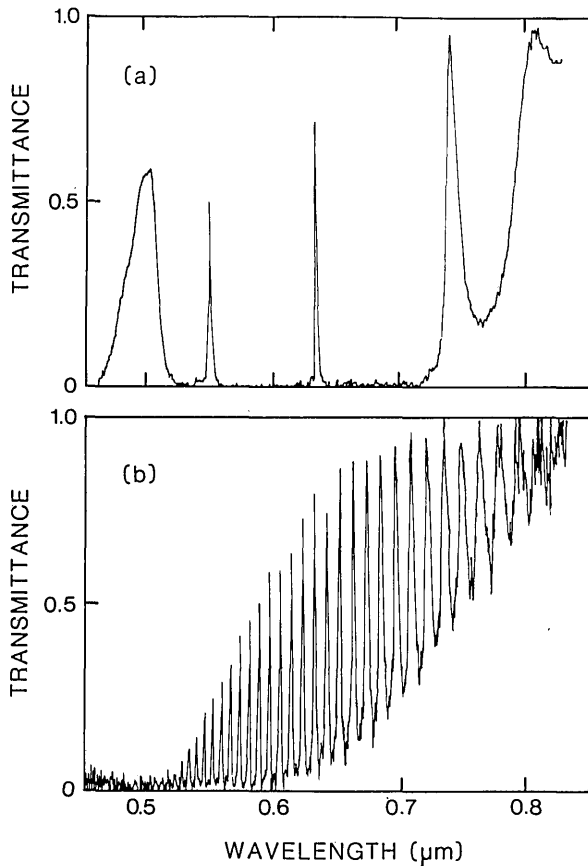


Fig. 1. (a) Transmission of narrow, bandpass filter with a 2λ optically thick spacer and four high-low layers in each reflective stack. (b) Transmission of a filter with a $6.6\text{-}\mu\text{m}$ MB-grown spacer and two high-low layers per stack.

sion in the filters. The temperature dependence of the low-power laser transmission was used to obtain a measure of the thermo-optic coefficient $\partial n/\partial T$ for the material structure that pertains in the thin films.

The linear filter transmission coefficient T_r has the form

$$T_r = T_r(\text{peak}) (1 + F \sin^2\phi)^{-1}, \quad (1)$$

where the cavity finesse is $\pi F^{1/2}/2$ and the round-trip phase change in the spacer region is 2ϕ . The refractive-index changes are of order 1% or lower in the bistability experiments. $T_r(\text{peak})$ and F are effectively independent of temperature over the range of interest. The variation of T_r is dominated by that of the phase $\phi(T, \theta_0)$ at temperature T and incident angle θ_0 . Both the spacer optical path length and the phase change on reflection from the stacks must be accounted for in $\phi(T, \theta_0)$.

Using the He-Ne laser itself, at low power level, the temperature dependence of the irradiance angle at peak transmission θ_p gives a direct measure of $\partial n/\partial T$. Under peak conditions ϕ is constant ($= N\pi$). A numerical calculation gives the relative change in refractive index $\Delta n/n$ corresponding to the change in peak angle $\Delta\theta_p$, and hence we can deduce $\partial n/\partial T$.

From the experimental peak positions, we obtain, at 633 nm, $\partial n/\partial T = 2 \times 10^{-4} \text{ K}^{-1}$, using $n = 2.47$. By comparison, at 514 nm the data of Ref. 2 give $\partial n/\partial T = 2.3 \times 10^{-4} \text{ K}^{-1}$ ($n = 2.72$). This weak wavelength dependence is consistent with the broad ZnSe band tail in the filter material.

633- AND 647-nm OPTICAL BISTABILITY

Figure 2 shows the transmitted versus incident power levels for the thin-spacer filter at various sample orientations. The orientation determines the initial detuning, the value of ϕ at ambient temperature. For θ_0 less than 13° , the 633-nm line is initially on the short-wavelength side of the filter transmission peak, and the thermally induced increase in the ZnSe refractive index moves the peak to yet longer wavelengths with a corresponding decrease in the transmission coefficient. For θ_0 greater than 13° , T_r increases initially until the filter peak is swept through the operational wavelength. One achieves bistability for angles greater than 16.5° .

For a laser spot size ($1/e^2$ diameter) of $17 \mu\text{m}$ the critical power level, below which bistability is not observed, is 22.5 mW. The switching contrast from 12% transmission to 50% is a considerable improvement over that for 514-nm operation (which is typically from 10% transmission to 25%; see Ref. 1. The results of Fig. 2 were obtained by irradiating from the dielectric side; a slightly lower critical power (17

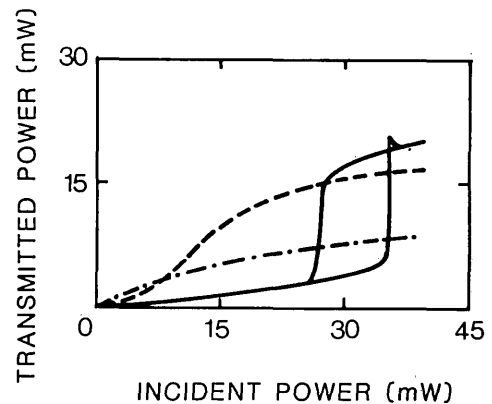


Fig. 2. Nonlinear response characteristics for the thin filter [Fig. 1(a)] for incident angles of 11.5° (dashed-dotted curve), 14.5° (dashed curve), and 16.5° (solid curve).

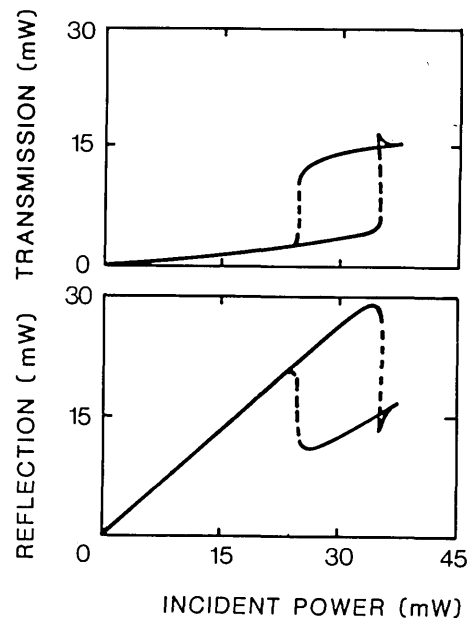


Fig. 3. Transmission and reflection optical bistability for the thin filter for illumination from the substrate side.

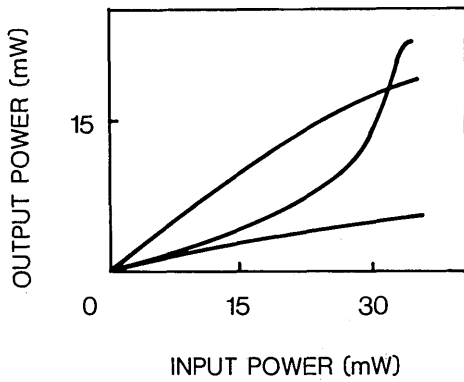


Fig. 4. Nonlinear response of 6.6- μm filter using He-Ne irradiation for three sample positions (i.e., at differing detunings).

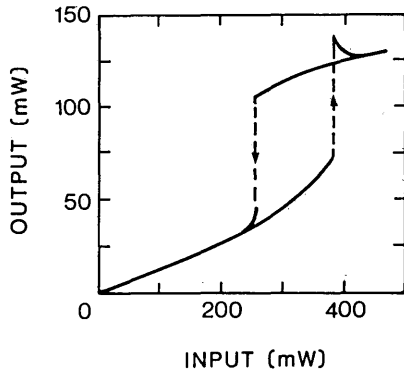


Fig. 5. Bistability at 647 nm in the 6.6- μm filter, using a cw Kr laser.

mW) and hysteric loops of improved stability are obtained by irradiation through the glass substrate (Fig. 3).

For the MB samples of spacer thicknesses 1.47–2.46 μm at 633 nm no optical nonlinearity was observed. For 4.3- and 6.6- μm spacers, however, one obtains strong nonlinearity, as is depicted in Fig. 4. Hysteresis is almost achieved at 30 mW for the 6.6- μm sample, using the He-Ne laser. As a consequence of these encouraging results, we obtained time on a cw Kr laser at the Royal Signals and Radar Establishment (R.S.R.E.), Malvern, United Kingdom. This system has a potential cw power of 4 W; the output consists of two lines at 647 and 676 nm in the power ratio of 4:1. The nonlinear transmission results for the 6.6- μm samples are shown in Fig. 5. Optical bistability is achieved at powers above 75 mW (and above 90 mW in the 4.3- μm sample). The figure is for a spot size of 40 μm ; on reduction to 30 μm the switch powers reduce to 55 and 80 mW, respectively, but the hysteresis loops are less stable.

NONLINEAR FABRY-PEROT ANALYSIS

An explanation of the above results is obtained from the considerations of Ref. 6. The form of the characteristic power level for the onset of switching is (at normal incidence)

$$P_c \approx \frac{\lambda_v \alpha \kappa_s r_0}{(\partial n / \partial T)} \frac{f(R_F, R_B, \alpha D)}{\alpha D}, \quad (2)$$

where λ_v is the radiation vacuum wavelength and κ_s is the substrate thermal conductivity; r_0 is the spot radius.

The key to low-power operation lies in the cavity factor, f /

αD . This factor has a pronounced minimum, as a function of αD , in the region $\alpha D = (2 - R_F - R_B)$. Here R_F and R_B refer to the front and back stack reflectivities. For radiation at an angle θ in the spacer, D is to be replaced by $D/\cos \theta$ in expression (2) and the stack reflectivities calculated for the appropriate angle. For the thin filter, $R_F \sim 0.96$ and $R_B \sim 0.94$. The MB filters were fabricated for optimum stack reflectivities at 510 nm. At 633 nm the calculated normal incidence reflectivities are, respectively, 0.53 and 0.44. Figure 6 shows the cavity factors in P_c for the above conditions. Parameters appropriate to various filters are marked. One sees clearly that a lower characteristic power level pertains in the thin sample and that of the MB samples the thickest should be the closest to optimum, in agreement with the experiments. A figure of merit for the cavities is

$$x = (2 - R_F - R_B)/\alpha D.$$

In the high-finesse limit the minimum cavity factor occurs at $x = 1$ and has a value that is independent of R_F, R_B . For nonoptimized cavities the switching power level will be increased with respect to the optimum by an amount of order $p = (x + 2)^3/27x$. Thus for the thin filter $x \approx 15.8$ and $p \approx 13$ and for the 6.6- μm sample $x \approx 22.0$ and $p \approx 23$.

To reduce the experimental switching power, it is evident that either higher-reflectivity stacks should be used or thicker spacers (or further reduction in beam spot size).

The dashed line in Fig. 6 corresponds to irradiation through the glass substrate in the thin-spacer sample. The slight improvement in this configuration is again in accord with experimental finding.

TEMPERATURE AND IRRADIANCE CONSIDERATIONS

Under 514-nm operating conditions, the temperature rise at switch point is in excess of 50 K and indeed has been quoted to be as high as 180 K. Now, the original purpose of using

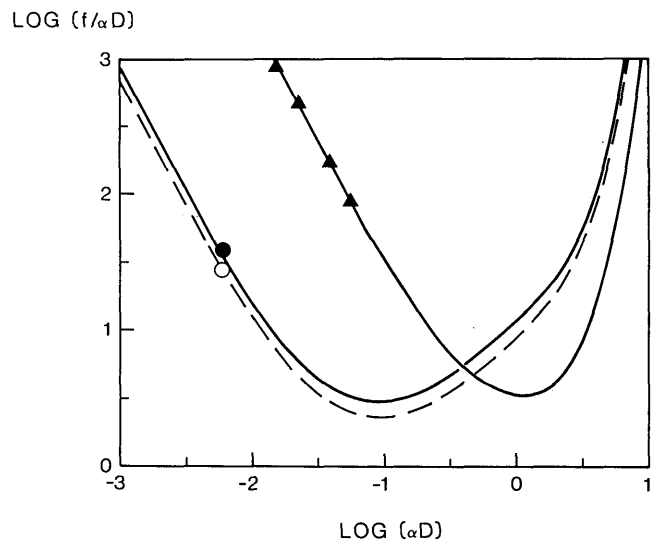


Fig. 6. The cavity factor $f/\alpha D$ in the critical power for bistability, calculated for filters with $M = 4$ and two high-low layers in each stack. The dashed line corresponds to irradiation from the substrate side for $M = 4$. Circles refer to the 633-nm thin-spacer sample and triangles to the various MB samples operated in the red spectral region.

Table 1. Switching Parameters for ZnSe-Based Nonlinear Étalons

Sample	Thin-Spacer Filters		MB Filters		Bulk ZnSe
Spacer length (μm)	~ 0.4	~ 0.5	1.7	6.6	360
Wavelength (nm)	514	633	514	647	476
Spot-size (μm) $1/e^2$ diameter	30	17	30	40	70
Cavity factor $f/\alpha D$	3	50	4	100	7
Material factor $\lambda_0 \alpha \kappa / (\partial n / \partial T)$	3.4	0.4	3.4	0.3	0.6
Predicted temperature rise on switching (K)	70	30	60	40	2
Predicted internal irradiance (kW cm^{-2})	8	70	1.4	3	0.14
Observed stability (qualitative)	Fairly unstable	Very unstable	Stable	Stable	Stable
Predicted switching power (mW)	15	17	20	60	16
Observed minimum switch power (mW)	16	20	35	60	15

514-nm operation with ZnSe was to take advantage of the proximity of the fundamental band gap both in providing absorption and in enhancing the thermo-optic coefficient. Using similar analyses to those at 633 nm, the absorption coefficient at 514 nm is of the order of 10^3 cm^{-1} and therefore gives $\alpha D \sim 0.04$ in 400-nm spacer layers and near-optimum conditions for filters with three high-low layer-pair stacks. However, the high-temperature rise produced leads to a movement of the band edge to longer wavelengths, and instability with associated thermal runaway can occur. Further, under optimum cavity conditions, one does not in practice obtain a large reduction in p_c near the band edge, because $\alpha/(\partial n/\partial T)$ does not decrease at the edge.⁶ Indeed, we find very much the same $\partial n/\partial T$ value at 633 nm as at 514 nm, even though α has decreased by a factor of 10. For these reasons, when results for the various thermally evaporated filters were compared, similar switch powers, but lower temperature rises and improved stability, were anticipated at 633 nm (Table 1).

Under critical conditions for 633-nm operation the temperature rise ΔT is approximately one half of that for 514-nm operation. However, the overall stability of the hysteresis loops is found to be very poor. If the irradiation is held above the switch point, then the loop drifts and narrows eventually to a nonhysteretic characteristic over a matter of seconds for 633-nm operation and longer for 514-nm samples. Permanent damage can then be observed. These instabilities are currently considered to be associated with the internal irradiance level. Table 1 shows experimental and calculated results that contrast the switching parameters for a number of filter structures. Notably for the thin-spacer filters, while lower temperature rises occur at 633 nm than at 514 nm, the internal irradiances are significantly higher at 633 nm.

We also note that reduction of the 633-nm beam diameter below $17 \mu\text{m}$ produces even more instability and that the critical power for bistability increases. A possible explanation for this is that the electronic contribution to the refrac-

tive-index change becomes more significant. As this has the opposite sign to $\partial n/\partial T$ it will reduce the size of the refractive-index change.⁶ For spot sizes greater than $17 \mu\text{m}$, P_c does scale linearly with r_0 as expected.²

One predicts the lowest switching irradiances to be in the MB filters (and in bulk ZnSe). We note that at 633 nm the MB responses, although not hysteretic, are invariant when held at 30-mW power levels for periods up to 1 h and at 647 nm the hysteretic responses are stable with only slight drift when repeatedly ramped around the hysteresis loop over a period of 90 min. No permanent damage was observed. Completely stable operation was previously reported in bulk ZnSe.⁹ In addition to their lower irradiance levels, the MB and bulk materials are likely to be inherently more stable. The spacer regions are dense and contain no porosity.¹⁰ In contrast, in the thin-spacer filters the conventional high-vacuum-deposition conditions are known to lead to porous layers.¹¹ This causes ingress of varying amounts of water from the atmosphere, which will be partially desorbed on subsequent heating. The instability of the thin filters may be, in part, attributable to this effect. A detailed experimental study of filter stability is currently being made.

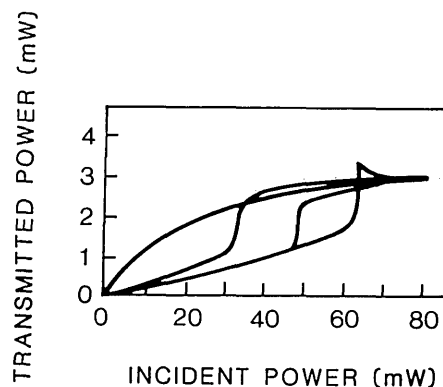


Fig. 7. 514-nm bistability in the 1.7- μm spacer filter for differing initial detunings.

514-nm BISTABILITY IN MOLECULAR-BEAM SAMPLES

The MB-filter stacks were designed for operation at 514 nm, with $R_F \approx 0.85$ and $R_B \approx 0.79$. The improved reflectivities and increased αD with respect to 633-nm operation do result in observation of optical bistability, at power levels of the order of 35 mW (30- μm spot size). At this wavelength all filters display bistable responses; the 1.7- μm sample gives the lowest critical power (Fig. 7). From the theoretical analysis this substantiates our conclusion that $\alpha \sim 1000 \text{ cm}^{-1}$ in the MB film and supports the cavity optimization procedure that we have used.

CONCLUSION

Optical bistability has been observed in both thin-film interference filters and filters with up to 6.6- μm MB-grown spacers. Critical power levels are consistent with the quasi-plane-wave model developed for cavity optimization of thermal refractive bistability. The cavity figure of merit $x = (2 - R_F - R_B)/\alpha D$ allows one to judge the power level required for a given cavity compared with that of an optimized cavity for which $x = 1$. To a first approximation, required power levels are proportional to $(x + 2)^3/(27x)$.

647-, 633-, and 514-nm studies of the MB samples indicate that bistability should be achievable at power levels between 20 and 50 mW over the full wavelength range for 30- μm spot sizes. Immediate proximity to the band edge is not essential, provided that the filter structure is close to optimum ($x \approx 1$) over the wavelength range.

Theoretical analyses indicate that the internal irradiance level must be kept low to prevent irreversible drift of the nonlinear responses. Such drift may be associated with morphological changes, but this is yet to be established.

ACKNOWLEDGMENTS

Y. T. Chow is grateful for support from the Croucher Foundation. Funding from the Procurement Executive of the Ministry of Defence, Directorate of Components, Valves and Devices, and from the Science and Engineering Research Council through the Joint Optoelectronics Research Scheme is acknowledged. We should like to thank A. M. Pitt of

R.S.R.E., Malvern, for assistance in the growth of the MB filters.

* Present address, Center of Applied Quantum Electronics, Department of Physics, North Texas State University, Denton, Texas.

† Present address, Royal Signals and Radar Establishment, Great Malvern, Worcester, United Kingdom.

REFERENCES

1. S. D. Smith, J. G. H. Mathew, M. R. Taghizadeh, A. C. Walker, B. S. Wherrett, and A. Hendry, "Room temperature, visible wavelength optical bistability in interference filters," *Opt. Commun.* **51**, 357-362 (1984).
2. I. Janossy, M. R. Taghizadeh, J. G. H. Mathew, and S. D. Smith, "Thermally induced optical bistability in thin-film devices," *IEEE J. Quantum Electron.* **QE-21**, 1447-1452 (1985).
3. F. V. Karpushko and G. V. Sinityn, "An optical logic element for integrated optics in a nonlinear semiconductor interferometer," *J. Appl. Spectrosc. (USSR)* **29**, 1323-1326 (1978).
4. D. A. Weinberger, H. M. Gibbs, C. F. Li, and M. C. Rushford, *J. Opt. Soc. Am.* **72**, 1769 (A) (1982).
5. G. R. Olbright, N. Peyghambarian, H. M. Gibbs, H. A. MacLeod, and F. Van Milligen, "Microseconds room-temperature optical bistability and cross-talk studies in ZnS and ZnSe interference filters with visible light and milliwatt powers," *Appl. Phys. Lett.* **45**, 1031-1033 (1984).
6. B. S. Wherrett, D. Hutchings, and D. Russell, "Optically bistable interference filters: optimization considerations," *J. Opt. Soc. Am.* **3**, 351-362 (1986).
7. K. L. Lewis and J. A. Savage, "A fundamental approach towards improved optical coatings," in *Proceedings of the Symposium on Laser Induced Damage in Optical Materials* (National Bureau of Standards, Washington, D.C., 1983).
8. K. L. Lewis and G. S. Arthur, "Surface and free carrier absorption processes on CVD zinc selenide," *Nat. Bur. Stand. Spec. Publ.* **669**, 86 (1984).
9. A. K. Kar and B. S. Wherrett, "Thermal dispersive optical bistability and absorptive bistability in bulk ZnSe," *J. Opt. Soc. Am.* **3**, 345-350 (1986).
10. K. L. Lewis, J. A. Savage, A. G. Guild, N. G. Chew, L. Charlwood, and D. W. Craig, "Assessment of optical coatings prepared by molecular beam techniques," in *Proceedings of the Symposium on Laser Induced Damage in Optical Materials* (National Bureau of Standards, Washington, D.C., 1984).
11. H. K. Dulker and E. Jung "Correlation between film structures and sorption behaviour of vapour deposited ZnS, cryolite and MgF_2 films," *Thin Solid Films* **9**, 57 (1971).